

# ERROR TOLERANCE CHARACTERIZATION FOR THE HUST MeV ULTRAFAST ELECTRON DIFFRACTION SYSTEM\*

Y. Song<sup>†</sup>, K. Fan, C.-Y. Tsai, Huazhong University of Science and Technology, Wuhan, China

## Abstract

Ultrafast electron diffraction (UED) is a powerful tool for probing atomic dynamics with a femtosecond resolution. Such a spatiotemporal resolution requires error tolerance for the UED system which includes the RF system, the laser system, the beamline elements, etc. To characterize the error tolerance of the required spatiotemporal resolution for the 1.4-cell MeV UED we are developing, we use ASTRA to simulate the UED model with errors including initial transverse beam centroid offset, RF amplitude jitter and injection phase jitter, etc. By performing simulations with different errors omitted, we can characterize the contribution of each error and thus set the tolerance for each error to obtain the required performance of UED experiment. In the end, we present the error tolerance for 10% emittance growth and 100 fs time of flight variation to maintain the required spatiotemporal resolution.

## INTRODUCTION

Ultrafast electron diffraction (UED) is a powerful pump-probe system which has shown promising potential in the last decades in investigating nano-structure dynamics with a femtosecond-level resolution [1-5]. Such a high spatiotemporal resolution requires setting of error tolerances which can be challenging in aspects of hardware and software. To perform a UED experiment, the normalized transverse emittance of electron beam (referred as transverse emittance hereby) needs to be small enough ( $<0.1 \pi$  mm-mrad) to obtain a sharp diffraction pattern which corresponds to the spatial resolution directly. The temporal resolution of UED is mainly limited by the time of flight (TOF) variation (between beam pulses) and bunch length of electron beam [6]. Since bunch length can be compressed by RF compressing cavity or other method [7, 8], we will focus on the TOF variation in the following discussion.

In this paper, we use ASTRA to simulate some possible error sources including initial transverse beam centroid offset, injection phase jitter, RF amplitude jitter, and beam charge jitter. By omitting certain error source, we can evaluate its contribution on concerned beam parameters which are the transverse emittance and TOF variation. By this method, we pinpointed the error sources that have the most contributions to emittance growth and TOF variation. First, the emittance growth is mostly the contribution of initial transverse beam centroid offset, which may be caused by laser misalignment or pointing jitter. Second, the TOF variation is mainly caused by RF amplitude jitter instead of injection phase jitter for 1.4-cell RF gun. Next, we

determine the relationship between emittance growth and initial transverse beam centroid offset (referred as beam centroid offset hereby) by ASTRA simulation and thus conclude the error tolerance for emittance growth less than 10%. For TOF variation, we analyse it by taking its first order derivative with respect to RF amplitude, injection phase and beam centroid offset to approximately evaluate their contribution and thus characterize the error tolerance for a 100fs or less TOF variation.

## ERROR SOURCES FOR 1.4-CELL UED

The simplified layout of the 1.4-cell HUST (Huazhong University of Science and Technology) MeV UED is presented in Fig. 1.

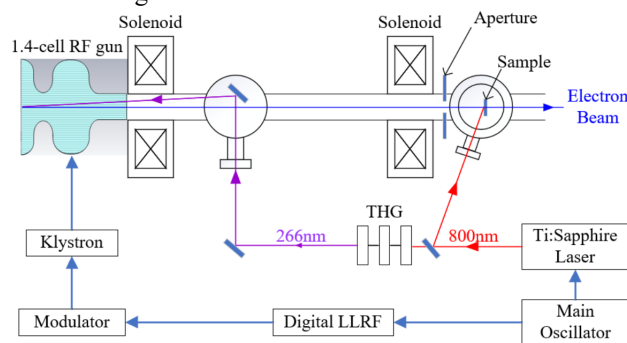


Figure 1: Layout of 1.4-cell HUST MeV UED.

The laser set up in Fig. 1 may have misalignment and pointing jitter on photocathode at the same time, which cause initial transverse beam centroid offset. The modulator produces pulsed high voltage on klystron with a 0.5% (RMS) pulse-to-pulse amplitude jitter, which also causes phase jitter of klystron once applied. Thus, the RF field in the 1.4-cell RF gun suffers from injection phase jitter and RF amplitude jitter. We assume that the RF amplitude jitter in RF gun is also 0.5% and the injection phase jitter 100fs according to other UED systems [9, 10]. The laser pulse-to-pulse energy jitter is below 0.5% (RMS) for the Ti: Sapphire laser we purchased [11]. We consider electron beam charge jitter equal to this pulse-to-pulse laser energy jitter. Besides, we presume that all the errors are random and Gaussian distributed and their rms values are summarized in Table 1.

Table 1: Error Sources

Error	RMS value
Beam centroid offset	0.5 mm
RF amplitude jitter	0.5%
Injection phase jitter	100 fs (0.103°)
Beam charge jitter	0.5%

\* Work supported by the National Natural Science Foundation of China (NSFC) 11728508

<sup>†</sup> d201780370@hust.edu.cn

Some RMS values of errors are undetermined and thus set relatively large to be on the conservative side. Error sources like solenoid field jitter and rotation error are beyond the scope of this paper.

## ERROR SIMULATION

### Simulation Method

The 1.4-cell HUST MeV UED model we use includes space charge effect, which make it difficult to evaluate its error sources analytically. Hence, we use the ERROR namelist in ASTRA. ERROR namelist gives each initial parameter a random Gaussian distributed error according to Table 1. The description and initial parameters of the UED model we used for simulation are presented in Ref. [12].

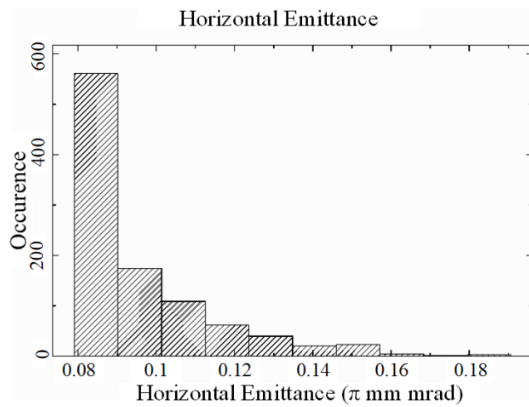


Figure 2: Occurrence distribution of transverse emittance values for 1000 times repetition with all error sources.

By 1000 times repetition, the random Gaussian distributed initial parameters will cause random distributed beam parameters as shown in Fig. 2 for example. The emittance of the most occurrence, which is about 0.08  $\pi$  mm·mrad, corresponds to the situation without any errors. The emittance in Fig. 2 varies from 0.08  $\pi$  mm·mrad to 0.18  $\pi$  mm·mrad approximately. This 125% relative variation corresponds to the contribution of all the errors included in the simulation.

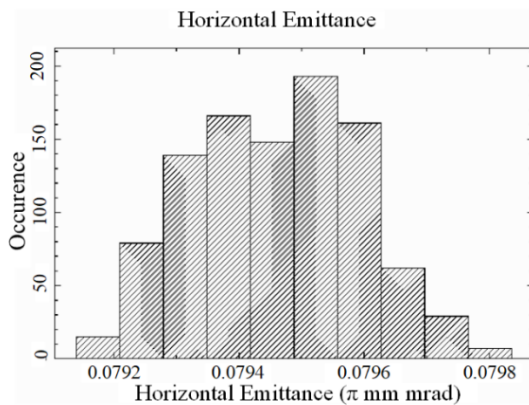


Figure 3: Occurrence distribution of transverse emittance values for 1000 times repetition with all errors except for beam centroid offset.

Figure 3 shows the simulation result with only the beam centroid offset omitted. As shown in Fig. 3, the variation range of transverse emittance shrinks drastically which indicates that the beam centroid offset is the main contributor to the emittance growth in this case while other errors merely vary the transverse emittance less than  $\pm 1\%$ . Hence to confine the emittance growth within 10%, the beam centroid offset is the main factor to control.

### Simulation Results

Similar simulations are performed with other beam parameters. Here we only discuss the transverse emittance and TOF and the main contributors to their variation. The results are summarized in Fig. 4 and Fig. 5.

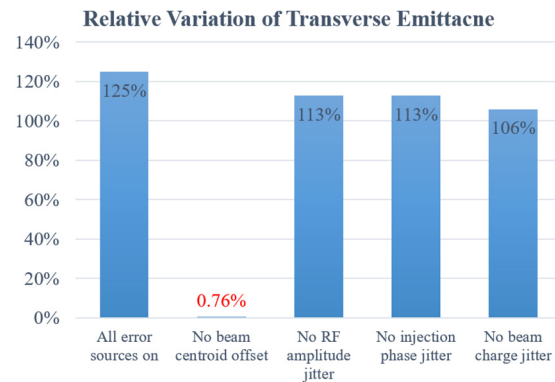


Figure 4: Relative variation of transverse emittance with different error settings.

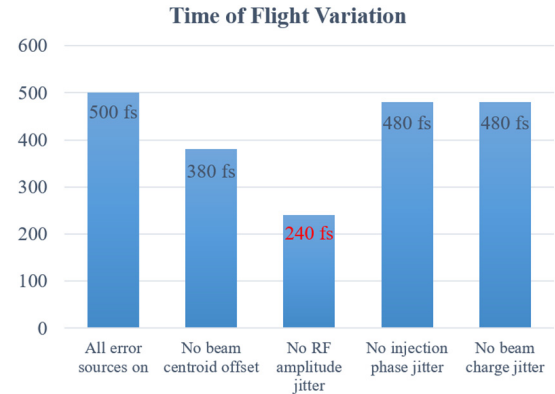


Figure 5: TOF variation with different error settings.

In Fig. 4, with all error sources considered, the transverse emittance grows 125% which can also be seen in Fig. 2. However, with beam centroid offset omitted, emittance growth (0.76%) almost disappears. In comparison, omitting other error sources show little suppression on the emittance growth, which indicates that we cannot confine the emittance growth by confining said error sources. Figure 5 indicates that the RF amplitude jitter is the main contributor to TOF variation while injection phase jitter shows almost no contribution. This phenomenon will be explained in the next section. Moreover, the beam centroid offset alters the trajectory of the beam centroid and thus contributes to the TOF variation while beam charge jitter shows almost no contribution to TOF variation since it basically has no influence on the beam centroid trajectory.

## ERROR TOLERANCE ANALYSIS

In the previous section, we found that the beam centroid offset contributes to the emittance growth and TOF variation. Hence by limiting the beam centroid offset, we can confine the emittance growth and TOF variation in the meantime. The emittance growth as a function of beam centroid offset is presented in Fig. 6, which indicates the RMS of beam centroid offset should be less than 100  $\mu\text{m}$  to confine the emittance growth within 10%.

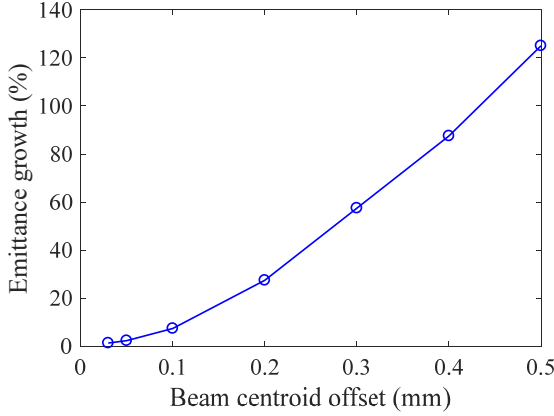


Figure 6: Emittance growth vs. beam centroid offset.

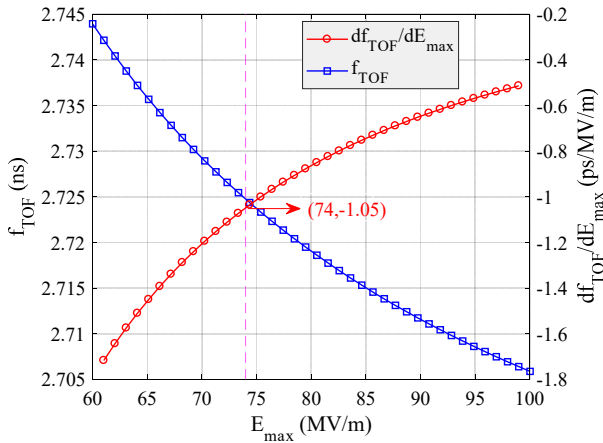


Figure 7: TOF as function of  $E_{\text{max}}$  (blue block) and the first derivative of TOF (red circle).

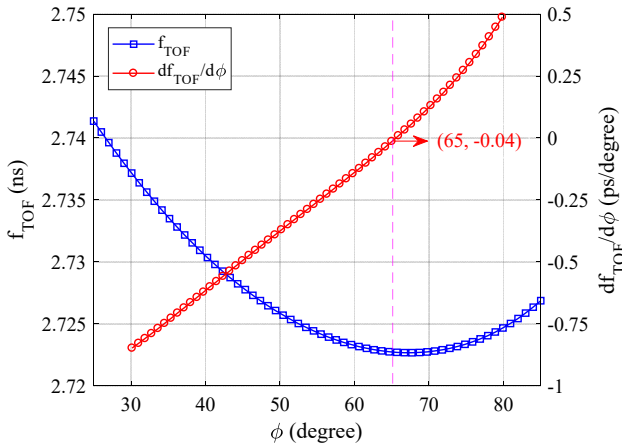


Figure 8: TOF as function of injection phase  $\phi$  (blue block) and the first derivative of TOF (red circle).

Since beam centroid offset is limited to a small value to confine emittance growth and the RF amplitude jitter and injection phase jitter are very small, we take the first-order total differential to evaluate their contributions to TOF variation as shown in Eq. (1).

$$df_{TOF} \approx \frac{\partial f_{TOF}}{\partial E_{\text{max}}} dE_{\text{max}} + \frac{\partial f_{TOF}}{\partial \phi} d\phi + \frac{\partial f_{TOF}}{\partial r} dr \quad (1)$$

Where  $f_{TOF}$  is TOF as a function of RF amplitude  $E_{\text{max}}$ , injection phase  $\phi$  and beam centroid offset  $r$ .

We present the TOF as the function of RF amplitude and injection phase in Fig. 7 and Fig. 8 respectively. The results are obtained by ASTRA from which we can also calculate the partial derivatives. The working point for the 1.4-cell HUST MeV UED is  $E_{\text{max}}=74$  MV/m with  $\phi=65^\circ$ .

As we can see in Fig. 8, we have

$$\left. \frac{\partial f_{TOF}}{\partial \phi} \right|_{\phi=65^\circ} = -0.04 \text{ ps / deg} \approx 0,$$

which explains why  $0.103^\circ$  injection phase jitter has almost no contribution to TOF variation as mentioned before.

Considering the symmetry of  $f_{TOF}$  around  $r=0$ , we have

$$\left. \frac{\partial f_{TOF}}{\partial r} \right|_{r=0} = 0,$$

Thus, Eq. (1) is reduced to Eq. (2) which indicates a linear relation between TOF variation and RF amplitude jitter. Such a relation has also been used in Ref. [13].

$$df_{TOF} \approx \frac{\partial f_{TOF}}{\partial E_{\text{max}}} dE_{\text{max}} = -1.05 \left[ \frac{\text{ps}}{\text{MV/m}} \right] dE_{\text{max}} \quad (2)$$

From Eq. (2) we can calculate the maximum RF amplitude jitter in theory for 100 fs TOF variation is 0.095 MV/m, which is 0.13% for 74 MV/m.

## SUMMARY

In this paper, we use ERROR simulation of ASTRA to pinpoint the error sources that have main contributions to emittance growth and TOF variation, which are the two main factors leading to the reduction of spatiotemporal resolution of UED system. We found that the beam centroid offset caused by laser misalignment and pointing jitter is the sole error that causes significant emittance growth and TOF variation is mainly caused by RF amplitude jitter rather than RF-to-laser phase jitter for 1.4-cell RF gun. By simulation and first-order analysis, we studied the error tolerance for 10% emittance growth and 100 fs TOF variation, which are initial beam centroid offset less than 100  $\mu\text{m}$  and RF amplitude jitter below 0.13%.

## REFERENCE

- [1] Y. Giret *et al.* “Determination of transient atomic structure of laser-excited materials from time-resolved diffraction data” *Appl. Phys. Lett.*, 103, 253107, 2013.  
doi: 10.1063/1.4847695
- [2] J. Yang, Y. Yoshida, H. Yasuda, “Ultrafast electron microscopy with relativistic femtosecond electron pulses”, *Microscopy*, 67, p291-295, 2018.  
doi: 10.1093/jmicro/dfy032
- [3] P. Musumeci *et al.* “Laser-induced melting of a single crystal gold sample by time-resolved ultrafast relativistic electron diffraction”, *Applied Physics Letters*, vol. 97, no.6, p.65, 2010. doi:10.1063/1.3478005
- [4] M. Gao *et al.* “Mapping molecular motions leading to charge delocalization with ultrabright electrons”, *Nature*, vol. 496, p.343, Apr. 2013. doi:10.1038/nature12044
- [5] A. W. P. Fitzpatrick, S. T. Park, and A. H. Zewail, “Exceptional rigidity and biomechanics of amyloid revealed by 4D electron microscopy”, in *Proc. National Academy of Sciences of the United States of America*, vol. 110, no. 27, p. 10976—10981, 27, Jul. 2013.  
doi: 10.1073/pnas.1309690110
- [6] J. C. Williamson, A. H. Zewail, “Ultrafast electron diffraction. Velocity mismatch and temporal resolution in crossed-beam experiments”, *Chemical Physics Letters*, vol. 209, p.10-16, Jun. 1993.  
doi: 10.1016/0009-2614(93)87193-7
- [7] J-H, Han, “Production of a sub-10 fs electron beam with 10<sup>7</sup> electrons”, *Phys. Rev. Accel. Beams*, vol. 14, p. 050101. 2011. doi: 10.1103/PhysRevSTAB.14.050101
- [8] C. Lu *et al.* “Coulomb-Driven Relativistic Electron Beam Compression”, *Phys. Rev. Lett.*, vol. 120, no.4, p. 044801, 2018. doi: 10.1103/PhysRevLett.120.044801
- [9] P. Zhu *et al.* “Femtosecond time-resolved MeV electron diffraction”, *New Journal of Physics*, vol. 17, no. 6, 2015.  
doi: 10.1088/1367-2630/17/6/063004
- [10] F. Fu *et al.* “High quality single shot ultrafast MeV electron diffraction from a photocathode radio-frequency gun”, *Review of Scientific Instruments*, vol. 85, p. 65, 2014.  
doi: 10.1063/1.4892135
- [11] <http://www.coherent.com/lasers/asterella-ultrafast-tisapphire-amplifier>
- [12] Y. Song, C-Y. Tsai, K. Fan, T. Yang and J Yang, “Improvement of 6D Brightness by a 1.4-cell Photocathode RF Gun for MeV Ultrafast Electron Diffraction” in *Proc. 10th Int. Particle Accelerator Conf. (IPAC'19)*, Melbourne, Australia, Apr.-May 2019, pp. 2033-2035.  
doi:10.18429/JACoW-IPAC2019-TUPTS047
- [13] R-K. Li and C-X. Tang, “Temporal resolution of MeV ultrafast electron diffraction based on a photocathode RF gun”, *Nucl. Instrum. Meth. Phys. Res. A*, vol. 605, p. 243-248. 2009, doi: 10.1016/j.nima.2009.03.236